

Published in final edited form as:

Exp Brain Res. 2009 July ; 196(4): 545–556. doi:10.1007/s00221-009-1885-3.

Cocaine- and amphetamine-regulated transcript (CART) peptide immunoreactivity in the brain of the CCK-1 receptor deficient obese OLETF rat

Hajnalka Abraham^{1,*}, Mihai Covasa², and Andras Hajnal³

¹Central Electron Microscopic Laboratory, Faculty of Medicine, University of Pecs, 7624 Pecs, Hungary

²Department of Nutritional Sciences, The Pennsylvania State University, University Park, PA 16802

³Department of Neural and Behavioral Sciences, The Pennsylvania State University, College of Medicine, Hershey, PA 17033

Abstract

Cocaine- and amphetamine regulated transcript (CART) peptide is expressed in brain areas involved in homeostatic regulation and reward. CART has been shown to reduce food intake but the underlying mechanisms and the relevance of this effect to obesity yet remain unknown. Therefore, we used immunohistochemistry to investigate expression of CART peptide in various brain regions of the obese Otsuka Long Evans Tokushima Fatty (OLETF) rats lacking the CCK-1 receptor. Analysis revealed that whereas the distribution of CART peptide-immunoreactive neurons and axonal networks was identical in OLETF rats and lean controls, intensity of CART immunoreactivity was significantly reduced in the rostral part of the nucleus accumbens ($p < 0.01$), the basolateral complex of the amygdala ($p < 0.05$), and the rostro-medial nucleus of solitary tract ($p < 0.001$) of the OLETF rats. These areas are involved in reward and integration of taste and viscerosensory information and have been previously associated with altered functions in this strain. The findings suggest that in addition to previously described deficits in peripheral satiety signals and augmented orexigenic regulation, the anorectic effect of CART peptide may also be diminished in OLETF rats.

Keywords

central food intake control; energy homeostasis; dietary obesity; type-2 diabetes; taste; food reward

Introduction

Regulatory mechanisms that are potential pharmacological targets for weight reduction are of great interest due to the alarmingly increasing trend of prevalence of obesity in the western countries. Recent work in our laboratory has focused on the Otsuka Long Evans Tokushima Fatty (OLETF) rat that has a mutation in the cholecystokinin (CCK)-1 receptor due to spontaneous deletion spanning the region from promoter to second exon of the CCK-1 receptor (CCK-1R) gene (Takiguchi et al. 1997). The lack of activity in this receptor

*Corresponding author: Hajnalka Ábrahám, M.D., Ph.D., Associate Professor, Central Electron Microscopic Laboratory, Faculty of Medicine, University of Pécs, 7643 Pécs, Szigeti u. 12. Hungary, Postal address: Pécs, 7602, P.O. Box. 99. Hungary, Tel.: 36-72-536-001 ext. 1511; Fax: 36-72-536-001 ext. 1510, hajnalka.abraham@aok.pte.hu.

is critical for the biological action of CCK on satiety (Moran 2000). OLETF rats have reduced satiety, increased meal size, and they gradually become obese and develop type-2 diabetes (Kawano et al. 1992; Moran 2000). In concert with this behavioral phenotype, recent studies have demonstrated alterations in central orexigenic systems regulating motivation for eating in this strain. Specifically, neuropeptide Y (NPY) expression in the dorsomedial nucleus of hypothalamus (DM) is higher in the OLETF than in Long Evans Tokushima Otsuka (LETO) lean control and this has been functionally linked to the hyperphagic trait (Bi et al. 2007). In addition, we recently showed altered synaptic dopamine regulation in the nucleus accumbens (NACC) of the OLETF rats (Anderzhanova 2007) and demonstrated a functional relationship between these alterations and a differential sensitivity to dopamine receptor antagonists and agonists on intake, preference and operant performance for palatable sucrose solution (Hajnal et al. 2007a, 2007b). Thus, it appears that in the OLETF rat, similar to individuals sensitive to dietary obesity, the integration of meal-size regulating signals fails. Despite this relationship, scarce data investigating anorexigenic systems, other than CCK, exists in the OLETF rats.

One such regulatory candidate well positioned to contribute to the above interactions is the putative peptide neuromodulator, the cocaine- and amphetamine regulated transcript (CART) peptide (Douglass and Daoud 1996; Smith et al. 1997). In addition to its anorectic action in various acute tests and models (for review see Vicentic and Jones 2007), human CART gene is a positional candidate for obesity (Echwald et al. 1999) and reduced CART signaling is manifested in obesity (Asnicar et al. 2001; Wierup et al. 2005). In the rat, CART peptide is present in hypothalamic areas relevant to feeding such as the arcuate and paraventricular nuclei and lateral hypothalamus (Koylu et al. 1997) and is expressed in perikarya and axons of forebrain areas including those responsible for reward and reinforcement (Koylu et al. 1998; Kozicz 2003; Philpot and Smith 2006; Seress et al. 2004). In the hindbrain, areas that play a primary role in viscerosensory/orosensory integration and reward functions also strongly express CART peptide, namely the commissural nucleus of the solitary tract (NTS) and the adjacent area postrema, and the parabrachial nucleus (PBN) (Koylu et al. 1998; Zheng et al. 2002). The CART-immunoreactive rich fiber plexus of the NTS originates mainly in the nodose ganglia which neurons also express CART peptide. It is notable that CART peptide is colocalized with CCK- 1R (Broberger et al. 1999) and injections of CART into the 4th ventricle strongly suppressed sucrose intake and stimulated expression of c-fos in the NTS (Zheng et al. 2002) similar to what has been reported for CCK (Fan et al. 2004).

Based on this evidence we hypothesized that CART signaling is altered in the hyperphagic OLETF rat. We assumed that if diminished CART expression is associated with OLETF's hyperphagic phenotype, it would suggest a causal relationship; whereas an upregulated expression of CART peptide would be indicative of a counter regulatory response. Thus, the present study aimed at investigating the anatomical distribution and intensity of CART peptide immunoreactivity in various brain areas related to feeding and reward in obese OLETF rats compared with age-matched lean LETO rats.

Materials and methods

Male OLETF (n=4, 35–40 weeks old) and LETO (n=5, 34–39 weeks old) rats were obtained as a generous gift of the Tokushima Research Institute, Otsuka Pharmaceutical, Tokushima, Japan. Rats were individually housed, maintained on a 12:12-hour light-dark cycle (lights on at 06:00, off at 18:00 hours) and received *ad libitum* tap water and pelleted rat chow (Teklad 2018). All protocols used were conducted in accordance with the National Institute of Health Guide for the Care and Use of Laboratory Animals (NIH Publications No. 80-23)

revised 1996 and approved by The Pennsylvania State University Institutional Animal Care and Use Committee.

Body weight was measured weekly and an oral glucose tolerance test (OGTT) was performed at 34 weeks of age to determine diabetic status. Following a 16 hours fast, an oral glucose load (2g/kg) was delivered to each rat via latex gavage. Blood glucose was measured before and at 30, 60, 90, and 120 minutes post-glucose loading using a standard glucometer (LifeScan, One-Touch Basic). Animals were classified as diabetic if the peak level of plasma glucose was ≥ 300 mg/dl or 16.66 mmol/l and a peak glucose level at 120 minutes > 200 mg/dl or 11.11 mmol/l (Kawano et al. 1992).

Rats were sacrificed and brain tissue was processed for immunohistochemistry as previously described (Seress et al. 2004). Briefly, after perfusion with ice cold phosphate buffer (PB, 0.1M pH 7.4) fixation was performed with cold 4% paraformaldehyde diluted in PB. After removal from the skull brains were postfixed in the same fixative used for the perfusion overnight for an additional 15–16 hours then 60 μ m coronal sections were cut with a vibratome. Following pretreatment with 1% hydrogen peroxide diluted in PB free floating sections were preincubated in normal horse serum (1%, Vector Laboratories, Burlingame, CA) diluted in PB containing 0.4% Triton-X 100 (Sigma) for 1 hour. This was followed by overnight incubation with primary rabbit anti-CART peptide antibody (1:10000) raised against CART (55–102) (Phoenix Pharmaceuticals, Belmont, CA) at room temperature. Binding sites were visualized with biotinylated secondary antibody (1:100, Vector Laboratories, Burlingame, CA) and the avidin-biotin peroxidase detection system (1:50, Vector Laboratories, Burlingame, CA) using 3,3'-diaminobenzidine (DAB) as chromogene.

The specificity and cross reactivity of anti-CART antibody has been determined by the company (Phoenix Pharmaceuticals, Belmont, CA). Regardless, CART peptide immunoreactivity obtained in lean control LETO rats with anti-CART (55–102) antibody was compared to CART peptide immunoreaction of two other, commercially not available CART peptide antibodies, which were previously also used in other studies in out-bred Long Evans and Sprague-Dawley strains (Koylu et al. 1997; Seress et al. 2004; Abraham et al. 2007). These were the primary monoclonal mouse anti-CART antibody prepared against purified recombinant CART (41–89) (Ca6-1 F4D4, a generous gift from Dr. J.T. Clausen, Novo Nordisk A/S, Bagverd, Denmark) and the primary polyclonal rabbit anti-CART antibody raised against another sequence of the CART peptide (79–102) (CART C4 12D, a generous gift from Dr. M.J. Kuhar, Division of Neuroscience, Yerkes National Primate Center of Emory University, Atlanta, GA). In addition, when primary antibody was omitted from our samples no immunostaining was observed.

Areas related to feeding and reward functions such as the hypothalamus, NACC, nuclei of amygdala, ventral pallidum, ventral tegmental area (VTA), PBN and NTS were digitally photographed with an Olympus BX51 microscope. Intensity of immunostaining was determined on black-and-white images using AnalySIS software.

In each animal and for each area 5–14 measurements were taken on the antero-posterior extension of the measured area, in non-consecutive sections. Intensity of immunoreactive area and the surrounding background intensity were measured in each section. Because CART peptide is released at the synaptic terminals (Smith et al. 1997), the staining intensity of white matter tracts located on the same section and lacking CART immunoreactivity was considered and measured as background intensity. During one single measurement staining intensity of 100 – 500 points of the background and 2000 – 6000 points of the region of interest was measured. Absolute gray-value intensity of the background was calculated by averaging the intensity values of the 100 – 500 measured points of the background.

Similarly, the average of the intensity values of the 2000 – 6000 measured points of the region of interest was calculated as absolute gray value intensity of the examined region. Relative gray-value intensity, referred as “gray-value intensity”, was calculated by subtracting absolute gray-value intensity of the region of interest from absolute gray-value intensity of the background. Since the light intensity of the visual field and the magnification used greatly affect the point-values as well as the gray-value intensity both of region of interest and its background, all measurements of one region of interest in both LETO and OLETF rats were done in one session using the same light and the same objective (20x) for magnification.

Body weight and blood glucose concentrations were compared using planned t-tests. For gray-value intensity, the average and the standard error were calculated for each area and statistical significance was determined using Student’s t-test. All data were expressed as means + SEM. Differences were considered statistically significant if $P < 0.05$. Statistical analyses were computed with Statistica software for PC (Version 6.1.; StatSoft inc., Tulsa, OK).

Results

Body weight and oral glucose tolerance test

When brains were harvested, OLETF rats were significantly heavier than age-matched LETO rats (638.4 ± 13.08 g vs. 500.6 ± 7.44 g for OLETF and LETO rats, respectively; $p < 0.05$). OGTT test showed elevated fasting glucose levels (6.20 ± 0.30 mmol/l, $p < 0.05$), a marked increase in the peak responses (17.05 ± 0.86 mmol/l, $p < 0.001$), and significantly elevated glucose levels at 120 min (9.64 ± 0.99 mmol/l, $p < 0.05$) in OLETF rats. In contrast, blood glucose levels in the LETO rats were all within the normal range (fasting glucose levels: 4.25 ± 0.25 mmol/l, OGTT peak response: 9.10 ± 0.30 mmol/l, glucose at 120 min: 6.55 ± 0.35 mmol/l).

CART peptide immunoreactivity in the forebrain

Neurons of the olfactory bulb and primary olfactory cortical areas including piriform cortex (Fig. 1A,B) exhibited CART immunoreaction similar to that observed previously (Koylu et al. 1998).

In the striatum, the rostral part of NACC displayed strong immunoreactivity in LETO (Fig. 1A), whereas CART immunoreactivity was slightly weaker in OLETF rats (Fig. 1B). The caudal part of NACC was equally moderately stained in both LETO and OLETF rats (Fig. 1C,D). CART immunoreaction was also present in caudate-putamen, globus pallidus, claustrum and ventral pallidum with no substantial difference between strains (Fig. 1C–F).

Medial septum contained low number of immunostained fibers, while moderately dense network of CART-immunoreactive fibers was observed in lateral septum, especially in its ventral part in both LETO and OLETF rats (Fig. 2A–D). Septohippocampal nucleus revealed also dense network of fibers without any obvious difference in control lean and obese rats (Fig. 2A–D).

In the hypothalamus, similar to the original description in normal Sprague-Dawley rats (Koylu et al. 1997) and in out-bred Long Evans strain (Seress et al. 2004), several hypothalamic nuclei expressed CART peptide. Large numbers of immunoreactive neurons and fibers were observed in paraventricular, periventricular and arcuate nuclei in both LETO and OLETF rats (Fig. 3A–D). Strongly CART-immunopositive neurons were detected in the perifornical nucleus, and in the dorsomedial hypothalamus in both lean and obese animals (Fig. 3E–F). The anterior and lateral hypothalamic area as well as the ventromedial

hypothalamic nucleus expressed moderately dense CART peptide-immunopositive fibers that were similarly stained in both strains (Fig. 3A–D). The highest density of CART-immunoreactive fibers in the hypothalamus was observed in the medial eminence in both LETO and OLETF rats. In addition, zona incerta contained large numbers of CART-immunoreactive neurons detected in both strains (Fig. 3C–F).

Several nuclei of the amygdala displayed neuronal and axonal CART immunoreaction. Central, medial and posterior nuclei of amygdala contained mostly CART-immunopositive fibers, whereas in addition to fibers, CART peptide expressing neurons were seen in central, basolateral and cortical nuclei in both strains (Fig. 4A–B). While no visible difference in staining intensity was observed in central and medial nuclei between obese and lean animals, CART-immunoreactivity was apparently weaker in the rostral portion of basolateral amygdala nuclei in OLETF than in LETO (Fig. 4A–B).

In the hippocampal formation, a group of granule cells of the dentate gyrus and their axons contain CART peptide detectable with immunohistochemistry as observed earlier in out-bred Long Evans strains (Seress et al. 2004; Abraham et al. 2007). CART-immunoreactive granule cells were localized to the outer part of the suprapyramidal blade of granule cell layer in both OLETF and LETO rats (Fig. 4C–D), in concert with the previously published observations (Seress et al. 2004; Abraham et al. 2007). Pyramidal cells of the subicular complex and entorhinal cortex expressed strong CART peptide immunopositivity, and dense CART-immunoreactive axonal fiber plexus was observed in layer I of entorhinal cortex (Fig. 4E–F). Layer IV of primary somatosensory cortex contained large number of faintly stained immunoreactive neurons in addition to the CART-immunopositive axons (Fig. 4G–H). CART immunoreaction in these archi- and neocortical areas revealed no meaningful difference in staining intensity between OLETF and LETO rats.

In the distribution of CART-immunoreactive elements, no significant differences were observed in the forebrain of obese OLETF and lean control LETO rats.

CART peptide immunoreactivity in the midbrain

In the ventral tegmental area (VTA), low number of immunoreactive fibers was observed in both strains without any visible difference (Fig. 5A–B). Periaqueductal gray exhibited large number of stained fibers, and Edinger-Westphal nucleus contained numerous strongly CART peptide-immunoreactive neurons (Fig. 5A–B). Both pars reticulata and compacta of substantia nigra revealed dense CART peptide expressing axonal network both in LETO and OLETF rats (Fig. 5A–D). The distribution of immunoreactive cells and fibers, as well as their staining intensity did not significantly differ in the midbrain of the lean LETO and obese OLETF animals.

CART peptide immunoreactivity in the hindbrain

In the brainstem, PBN contained large number of immunopositive fibers and low number of neurons, whereas the medial PBN displayed more moderate immunoreaction in both strains (Fig. 5E–F). In the medulla oblongata, the medial NTS exhibited dense CART-immunoreactive fiber plexus (Fig. 6A–F), however, in LETO rats the staining intensity was stronger than in OLETF animals, especially in the rostral part of the NTS (Fig. 6A, B, E and F). In addition, nucleus ambiguus, inferior olive, C1 adrenaline cells and nucleus raphe obscurus contained moderately dense immunoreactive neurons and fiber network both in obese and lean strains (Fig. 6A–D).

Staining intensity of CART peptide immunoreactivity

Results of gray-value intensity was determined in selected forebrain, midbrain and hindbrain structures relevant to energy homeostasis, food intake control and reward processes, such as the arcuate nucleus, paraventricular nucleus of the hypothalamus, nuclei of amygdala, NACC, VTA, NTS, and PBN (Fig. 7). In the majority of the examined structures moderate but non-significant differences were detected in LETO and OLETF rats when gray-value intensity was measured. However, in the rostral portion of the NACC, the gray-value intensity was significantly lower ($p < 0.01$) in OLETF than in lean LETO controls. A similar pattern was noted in the amygdala with staining intensity being overall reduced in OLETF rats across all nuclei complexes (medial, central, basolateral) investigated. This strain difference, however, reached statistical significance only in the basolateral complex ($p < 0.05$). Further separation of sections containing rostral and caudal basolateral nuclei of amygdala revealed that the effect was carried by the more rostral aspects ($p < 0.02$) whereas a comparison limited to the caudal basolateral complex was not significant. Furthermore, the rostro-medial NTS, exhibited significantly lower ($p < 0.001$) gray-value intensity in OLETF compared to LETO rats, whereas caudal NTS was unaffected. In addition, lower intensity values were measured in the lateral and external lateral subdivisions of the PBN of OLETF than in LETO rats, although, the difference was not statistically significant. In contrast, gray-value intensity in the caudal portion of the NACC, ventral pallidum, paraventricular nucleus of OLETF rats revealed higher values than that of LETO controls; however the differences did not reach statistical significance.

Discussion

One of the major findings of the present study was that the overall distribution of CART peptide expression in obese OLETF rats lacking functional CCK-1R does not differ substantially from the non-mutant, lean LETO controls. The localization of CART-immunoreactive neurons and axons present in the brain areas of OLETF was similar to LETO rats and to that previously described in normal lean strains such as Sprague-Dawley and out-bred Long Evans (Koylu et al. 1997, 1998; Seress et al. 2004). Thus, it seems that sustained expression of CART is not critically dependent on functional CCK-1Rs. It has to be considered, however, that this result was obtained in adult animals with complications from obesity, dysfunctional regulation of glucose homeostasis, and other metabolic derangements (Kawano et al. 1992, 2006). The second main observation of this study was that the intensity of the CART immunoreaction was in several areas diminished in OLETF compared to LETO rats. A significantly decreased intensity of CART immunoreaction in OLETF was observed in the rostral shell of the NACC, the rostral basolateral amygdala, and in the rostro-medial portion of the NTS.

CART peptide modulates mesolimbic dopamine system and plays a role in food reward and reinforcement processes (Hunter et al. 2004; Koylu et al. 1997; Kuhar and Dall Vechia 1999; Tim et al. 1998). Accordingly, CART mRNA and protein are present in the NACC in rat (Douglass and Daoud 1996; Koylu et al. 1998). Similarly to these previously published results, we found dense plexus of CART-immunoreactive fibers and perikarya in NACC shell, whereas CART immunoreaction was far less intense in the core and the dorsal striatum. Our observation that the intensity of CART immunoreaction in the NACC shell was significantly reduced in OLETF relative to LETO rats is the first to show differential CART expression in a naturally occurring obese animal. A reduced CART expression was seen also in the amygdala of the OLETF rats, especially in the basolateral nuclei. This area has been involved in various aversive behaviors including taste aversion (Parker and Gillies 1995; Reilly and Bornova 2005). Although the exact mechanisms by which basolateral amygdala may participate in taste reward functions remain unknown, there is strong behavioral and anatomical evidence supporting such role (Louilot and Besson 2000; Lundy

et al. 2004; Reilly and Bornovalova 2005; Ramirez-Lugo et al. 2007). Therefore it is possible that altered CART regulation in the OLETF rats affecting both the nuclei of the amygdala and the NACC may contribute to altered taste and food reward functions demonstrated in this strain.

We found reduced CART immunoreactivity in the rostro-medial portion of the NTS in the OLETF rats. The NTS is the recipient of the vagal afferents bringing mechanoreceptive and chemoreceptive information from the upper part of the alimentary tract. The caudal extent and mid-portion of the NTS are primarily involved in viscerosensory integration, while the more rostral part encompasses the first central gustatory relay neurons (for a review, see Lundy et al. 2004). In rodents, parallel and reciprocal connections exist also between subregions of the NTS and the subregions of the pontine parabrachial nucleus (Whitehead 1990; Williams et al. 1996; Cho et al. 2002) with both projecting to the NACC (Lundy et al. 2004). Thus, a reduced density of CART immunoreaction in the lateral PBN, may be, at least in part, related with gustatory afferents from the hindbrain. Of functional relevance, is the fact that lateral PBN is involved in aversion and preference (Reilly and Trifunovic 2000; Zafra et al. 2002; Paues et al. 2006) and fourth ventricular administration of CART in rats can cause malaise, and may be involved in development of conditioned taste aversion (Aja et al. 2002).

Based on these considerations, our finding suggests that altered CART expression in the hindbrain of the OLETF rats may contribute to deficits in integration of gustatory and viscerosensory signaling that is critical for appropriate control of meal size. Whereas the present study is limited to an anatomical analysis of CART expression, future functional analysis is warranted on the potential compensatory changes or downstream alterations in other regulatory systems that contribute to the obese phenotype in the OLETF strain.

It is intriguing that an anorexigenic system fails to become upregulated in an animal that expresses positive energy balance, increased adiposity, as well as increased insulin and leptin levels. One may suppose that mechanisms either upstream to the stimulation of the CART system(s) might have failed (i.e. insensitivity of receptors or inability of peripheral information routes to engage anorexigenic circuitries) or downstream feedback (i.e. other hypothalamic peptides, or monoamine systems) is perturbed in the OLETF rats. Evidence exists in support of both scenarios. For example, stimulation of the vagal afferents by mechanoreceptive and nutrient-related (i.e. chemosensory) stimuli is greatly dependent on intact CCK signaling that is impaired in the OLETF rats (De Jonghe et al. 2005; Moran and Bi 2006). This, together with the co-expression of CART and CCK-1R mRNA in the nodose ganglion cells projecting to the NTS (Broberger et al. 1999) may fit well the scenario for unresponsive CART regulation in the NTS of the OLETF rats.

In conclusion, our findings based on intensity measures of CART immunoreaction suggest that OLETF may express deficits in CART peptide signaling in areas that are related to integration of viscerosensory signals and food reward functions. A reduced anorexigenic effect, or abolished compensatory activation, of the CART system may further contribute to sustained overeating and increase avidity of palatable meals in this model.

Acknowledgments

The authors wish to thank Otsuka Pharmaceutical Co. (Tokushima, Japan) for the generous donation of the OLETF and LETO animals used to perform this study. The authors also thank Mr. N. Acharya and Mrs. Nelli Horvath for their excellent assistance with the oral glucose tolerance tests and histology, respectively. This research was supported by National Institute of Diabetes & Digestive & Kidney Diseases Grant DK065709. Dr. Abraham was a recipient of Hungarian State Eötvös Scholarship.

References

- Ábrahám H, Czéh B, Fuchs E, et al. Mossy cells and different subpopulations of pyramidal neurons are immunoreactive for cocaine- and amphetamine-regulated transcript peptide in the hippocampal formation of non-human primates and tree shrew (*Tupaia belangeri*). *Neuroscience*. 2005; 136:231–240. [PubMed: 16181735]
- Ábrahám H, Orsi G, Seress L. Ontogeny of cocaine- and amphetamine-regulated transcript (CART) peptide and calbindin immunoreactivity in granule cells of the dentate gyrus in the rat. *Int J Dev Neurosci*. 2007; 25:265–274. [PubMed: 17616293]
- Aja S, Robinson BM, Mills KJ, et al. Fourth ventricular CART reduces food and water intake and produces a conditioned taste aversion in rats. *Behav Neurosci*. 2002; 116:918–921. [PubMed: 12369811]
- Anderzhanova E, Covasa M, Hajnal A. Altered basal and stimulated accumbens dopamine release in obese OLETF rats as a function of age and diabetic status. *Am J Physiol Regul Integr Comp Physiol*. 2007; 293:R603–661. [PubMed: 17553848]
- Asnicar MA, Smith DP, Yang DD, et al. Absence of cocaine- and amphetamine-regulated transcript results in mice fed a high caloric diet. *Endocrinology*. 2001; 142:4394–4400. [PubMed: 11564703]
- Bi S, Scott KA, Tamashiro KL, et al. Knockdown of dorsomedial hypothalamic NPY gene expression prevents hyperphagia and obesity of OLETF rats lacking CCK1 receptors. *Society for the Study of Ingestive Behavior: Annual Meeting*, vol 49, *Appetite*. 2007:279.
- Broberger C, Holmberg K, Kuhar MJ, et al. Cocaine- and amphetamine-regulated transcript in the rat vagus nerve: A putative mediator of cholecystokinin-induced satiety. *Proc Natl Acad Sci U S A*. 1999; 96:13506–13511. [PubMed: 10557351]
- Cho YK, Li CS, Smith DV. Gustatory projections from the nucleus of the solitary tract to the parabrachial nuclei in the hamster. *Chem Senses*. 2002; 27:81–90. [PubMed: 11751472]
- De Jonghe BC, Hajnal A, Covasa M. Increased oral and decreased intestinal sensitivity to sucrose in obese, prediabetic CCK-A receptor-deficient OLETF rats. *Am J Physiol Regul Integr Comp Physiol*. 2005; 288:R292–300. [PubMed: 15358606]
- Douglass J, Daoud S. Characterization of the human cDNA and genomic DNA encoding CART: a cocaine- and amphetamine-regulated transcript. *Gene*. 1996; 169:241–245. [PubMed: 8647455]
- Echwald SM, Sorensen TI, Andersen T, et al. Sequence variants in the human cocaine and amphetamine-regulated transcript (CART) gene in subjects with early onset obesity. *Obes Res*. 1999; 7:532–536. [PubMed: 10574510]
- Fan W, Ellacott KL, Halatchev IG, et al. Cholecystokinin-mediated suppression of feeding involves the brainstem melanocortin system. *Nat Neurosci*. 2004; 7:335–336. [PubMed: 15034587]
- Hajnal A, Acharya NK, Grigson PS, et al. Obese OLETF rats exhibit increased operant performance for palatable sucrose solutions and differential sensitivity to D2 receptor antagonism. *Am J Physiol Regul Integr Comp Physiol*. 2007
- Hajnal A, De Jonghe BC, Covasa M. Dopamine D2 receptors contribute to increased avidity for sucrose in obese rats lacking CCK-1 receptors. *Neuroscience*. 2007; 148:584–592. [PubMed: 17681694]
- Hunter RG, Philpot K, Vicentic A, et al. CART in feeding and obesity. *Trends Endocrinol Metab*. 2004; 15:454–459. [PubMed: 15519893]
- Kawano K, Hirashima T, Mori S, et al. Spontaneous long-term hyperglycemic rat with diabetic complications. Otsuka Long-Evans Tokushima Fatty (OLETF) strain. *Diabetes*. 1992; 41:1422–1428. [PubMed: 1397718]
- Koylu EO, Couceyro PR, Lambert PD, et al. Cocaine- and amphetamine-regulated transcript peptide immunohistochemical localization in the rat brain. *J Comp Neurol*. 1998; 391:115–132. [PubMed: 9527537]
- Koylu EO, Couceyro PR, Lambert PD, et al. Immunohistochemical localization of novel CART peptides in rat hypothalamus, pituitary and adrenal gland. *J Neuroendocrinol*. 1997; 9:823–833. [PubMed: 9419833]

- Kozicz T. Neurons colocalizing urocortin and cocaine and amphetamine-regulated transcript immunoreactivities are induced by acute lipopolysaccharide stress in the Edinger-Westphal nucleus in the rat. *Neuroscience*. 2003; 116:315–320. [PubMed: 12559087]
- Kuhar MJ, Dall Vechia SE. CART peptides: novel addiction- and feeding-related neuropeptides. *Trends Neurosci*. 1999; 22:316–320. [PubMed: 10370256]
- Louilot A, Besson C. Specificity of amygdalostriatal interactions in the involvement of mesencephalic dopaminergic neurons in affective perception. *Neuroscience*. 2000; 96:73–82. [PubMed: 10683412]
- Lundy, RFJ.; Norgren, R. Gustatory System. In: Paxinos, G., editor. *The Rat Nervous System*. Elsevier Academic Press; San Diego, CA: 2004. p. 891-921.
- Moran TH. Cholecystokinin and satiety: current perspectives. *Nutrition*. 2000; 16:858–865. [PubMed: 11054590]
- Moran TH, Bi S. Hyperphagia and obesity of OLETF rats lacking CCK1 receptors: developmental aspects. *Dev Psychobiol*. 2006; 48:360–367. [PubMed: 16770763]
- Onaivi ES, Bishop-Robinson C, Motley ED, et al. Neurobiological actions of cocaine in the hippocampus. *Ann N Y Acad Sci*. 1996; 801:76–94. [PubMed: 8959025]
- Parker LA, Gillies T. THC-induced place and taste aversions in Lewis and Sprague-Dawley rats. *Behav Neurosci*. 1995; 109:71–78. [PubMed: 7734082]
- Paues J, Mackerlova L, Blomqvist A. Expression of melanocortin-4 receptor by rat parabrachial neurons responsive to immune and aversive stimuli. *Neuroscience*. 2006; 141:287–297. [PubMed: 16730913]
- Philpot K, Smith Y. CART peptide and the mesolimbic dopamine system. *Peptides*. 2006; 27:1987–1992. [PubMed: 16759749]
- Ramirez-Lugo L, Nunez-Jaramillo L, Bermudez-Rattoni F. Taste memory formation: role of nucleus accumbens. *Chem Senses*. 2007; 32:93–97. [PubMed: 16914504]
- Reilly S, Bornovalova MA. Conditioned taste aversion and amygdala lesions in the rat: a critical review. *Neurosci Biobehav Rev*. 2005; 29:1067–1088. [PubMed: 15893375]
- Reilly S, Trifunovic R. Lateral parabrachial nucleus lesions in the rat: aversive and appetitive gustatory conditioning. *Brain Res Bull*. 2000; 52:269–278. [PubMed: 10856824]
- Seress L, Abraham H, Doczi T, et al. Cocaine- and amphetamine-regulated transcript peptide (CART) is a selective marker of rat granule cells and of human mossy cells in the hippocampal dentate gyrus. *Neuroscience*. 2004; 125:13–24. [PubMed: 15051141]
- Smith Y, Koylu EO, Couceyro P, et al. Ultrastructural localization of CART (cocaine- and amphetamine-regulated transcript) peptides in the nucleus accumbens of monkeys. *Synapse*. 1997; 27:90–94. [PubMed: 9268069]
- Tagiguchi S, Takata Y, Funakoshi A, et al. Disrupted cholecystokinin type-A receptor (CCKAR) gene in OLETF rats. *Gene*. 1997; 197:169–175. [PubMed: 9332364]
- Thim L, Kristensen P, Larsen PJ, et al. CART, a new anorectic peptide. *Int J Biochem Cell Biol*. 1998; 30:1281–1284. [PubMed: 9924797]
- Vicentic A, Jones DC. The CART (cocaine- and amphetamine-regulated transcript) system in appetite and drug addiction. *J Pharmacol Exp Ther*. 2007; 320:499–4506. [PubMed: 16840648]
- Whitehead MC. Subdivisions and neuron types of the nucleus of the solitary tract that project to the parabrachial nucleus in the hamster. *J Comp Neurol*. 1990; 301:554–574. [PubMed: 2177063]
- Wierup N, Richards WG, Bannon AW, et al. CART knock out mice have impaired insulin secretion and glucose intolerance, altered beta cell morphology and increased body weight. *Regul Pept*. 2005; 129:203–211. [PubMed: 15927717]
- Williams JB, Murphy DM, Reynolds KE, et al. Demonstration of a bilateral projection from the rostral nucleus of the solitary tract to the medial parabrachial nucleus in rat. *Brain Res*. 1996; 737:231–237. [PubMed: 8930370]
- Zafra MA, Simon MJ, Molina F, et al. The role of the external lateral parabrachial subnucleus in flavor preferences induced by predigested food administered intragastrically. *Brain Res*. 2002; 950:155–164. [PubMed: 12231240]

Zheng H, Patterson LM, Berthoud HR. CART in the dorsal vagal complex: sources of immunoreactivity and effects on Fos expression and food intake. *Brain Res.* 2002; 957:298–310. [PubMed: 12445972]

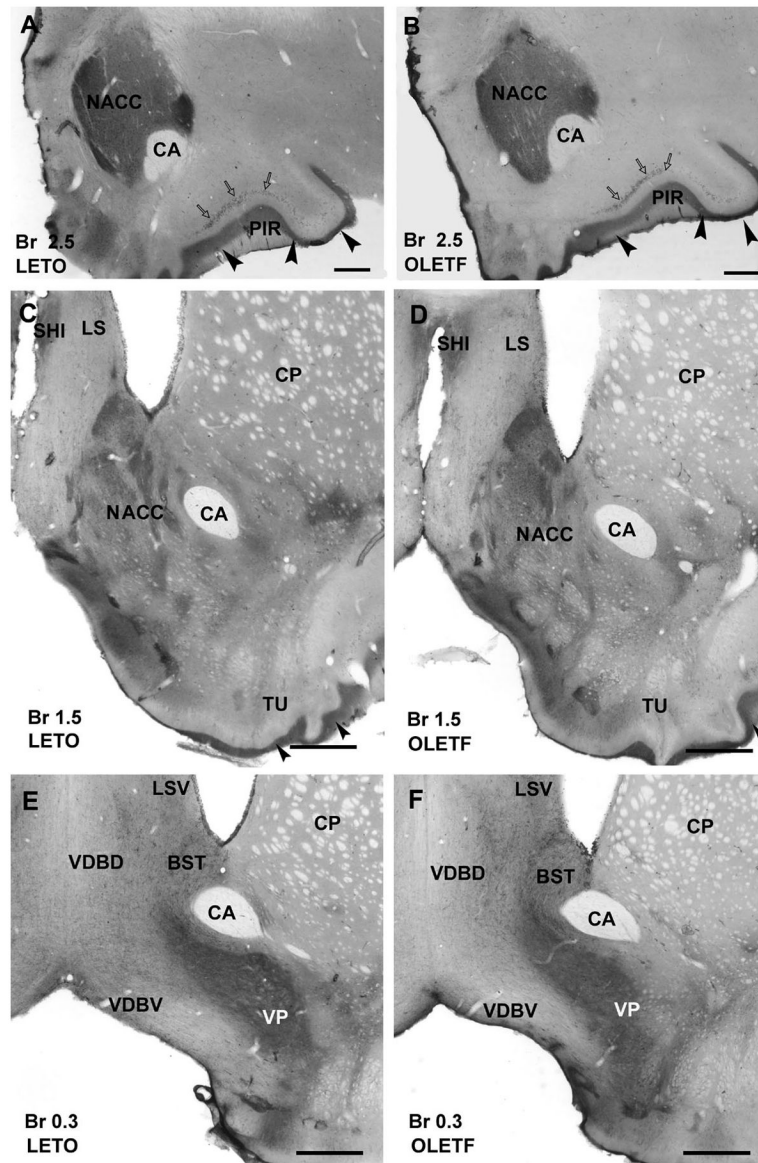


Figure 1. Photomicrographs illustrating CART-immunoreactive neuronal elements in the rostral part of forebrain in a lean LETO control (A, C, E) and obese OLETF rat (B, D, F). A: In LETO, dorsomedially to the anterior commissure (CA) the rostral portion of nucleus accumbens (NACC) shows a dense network of CART-immunoreactive fibers. In addition, densely packed immunoreactive axons are localized in layer I (arrowheads) of the piriform cortex (PIR) that also contains immunopositive neurons (open arrows). B: In OLETF, the rostral portion of nucleus accumbens (arrow) reveals slightly weaker immunoreaction than in LETO shown in A. Layers of of piriform cortex contain CART peptide-immunopositive neurons (open arrows) and a dense axonal plexus (arrowheads) similar to that found in LETO. C and D: No substantial difference is seen between the LETO (C) and OLETF strains (D) in the caudal part of nucleus accumbens which expresses moderate density of immunoreactive fibers and neurons. Olfactory tubercle (TU) reveals a dense network of immunoreactive fibers (arrowheads) in LETO (C) as well as in OLETF strains. In the lateral septum (LS) and in the septohippocampal nucleus (SHI) moderate density of

immunoreactive fibers is detected in both LETO (C) and OLETF (D) rats. Caudate-putamen (CP) contains very low number of CART immunoreactive neurons and axons in both strains (C and D). E and F: The bed nucleus of stria terminalis (BST) exhibits moderate numbers of immunostained neurons and fibers, while ventral pallidum (VP) contains high density of CART-immunoreactive fibers in both LETO (E) and OLETF (F) rats. The ventral part of lateral septum (LSV) expresses moderate immunoreactivity, the dorsal (VDBD) and ventral nucleus of vertical limb of diagonal band (VDBV) display loose networks of CART peptide-immunoreactive axons in both LETO (E) and OLETF (F) strains. Antero-posterior coordinates are represented in mm distance from the Bregma (Br). Scale bars = 500 μm in A and B, 600 μm in C–F.

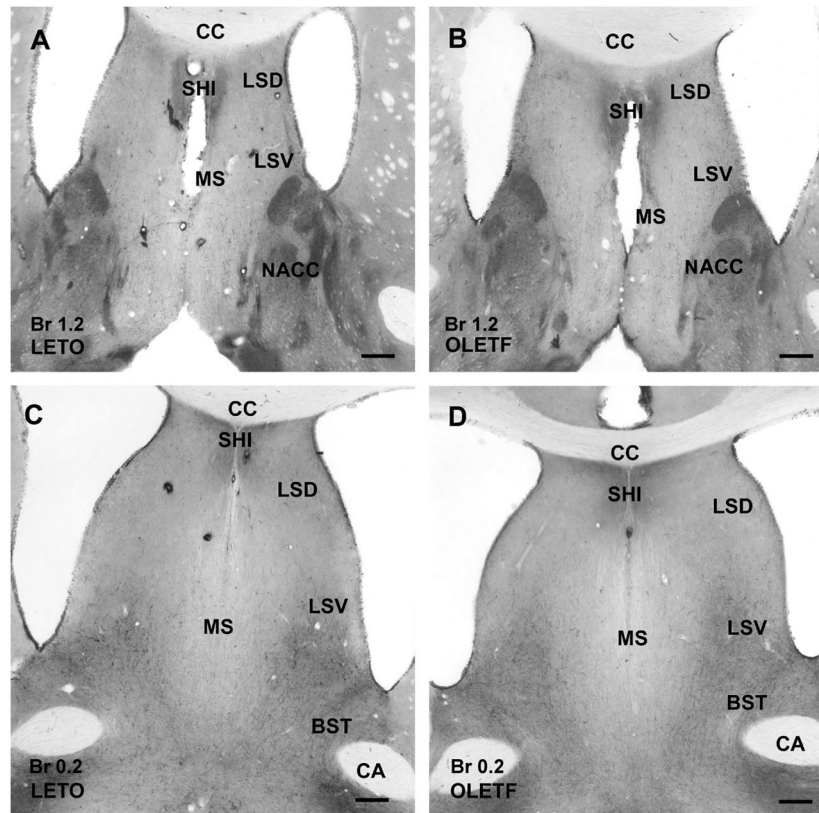


Figure 2. CART peptide immunoreaction in the septum of a lean LETO (A and C) and an obese OLETF (B and D) rat. A and B: The caudal part of septum contains a dense network of CART immunostained fibers in septohippocampal nucleus (SHI), while moderate density of immunoreactive fibers is visible in the dorsal (LSD) and ventral parts of lateral septum (LSV) in both LETO (A) and OLETF (B) rats. Medial septum (MS) contains very low density of immunoreactive elements. In contrast, nucleus accumbens (NACC) exhibits moderately dense immunoreactive fibers in both LETO (A) and OLETF (B) rats without substantial difference between the two strains. C and D: Similar to the cranial part of the septum, the caudal part of septohippocampal nucleus expresses relatively dense CART peptide-immunoreactive elements, the dorsal and ventral parts of the lateral septum contain moderately dense networks of immunostained fibers in both LETO (C) and OLETF (D) rats. Immunoreactivity is very low in the medial septum due to the loose network of fibers, while in the bed nucleus of stria terminalis (BST) moderate density of CART-immunopositive neurons and fibers are seen in both strains. Antero-posterior coordinates are represented in mm distance from the Bregma (Br). Additional abbreviations: CA, anterior commissure; cc, corpus callosum. Scale bars = 250 μm in A and B, 500 μm in C and D.

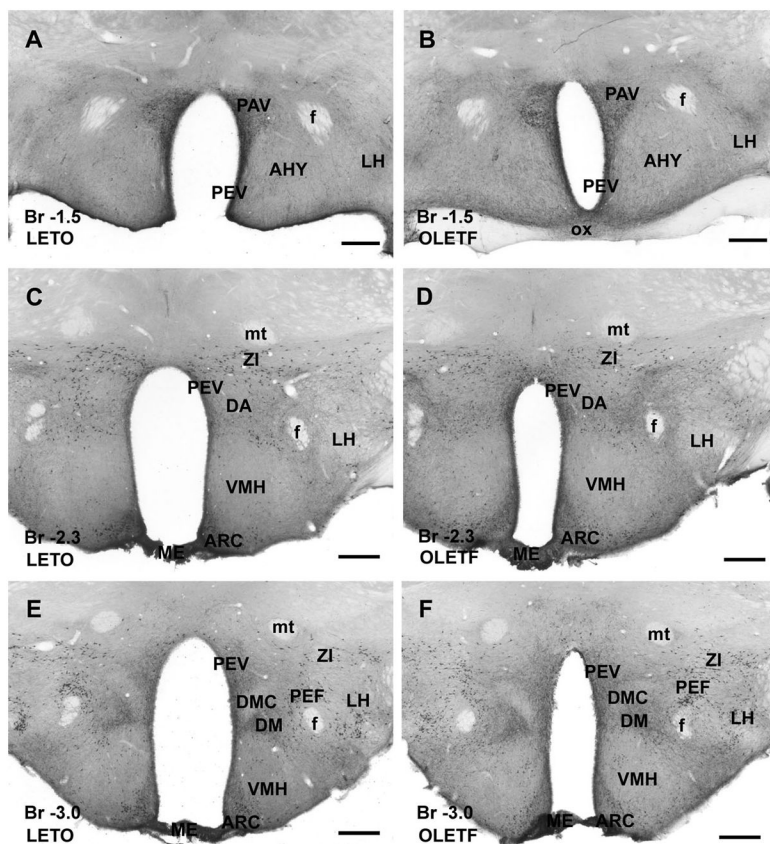


Figure 3. CART peptide immunoreaction in the hypothalamus of a lean control LETO (A, C and E) and an obese OLETF (B, D and F) rat. A and B: Rostrally, the paraventricular (PAV) and periventricular (PEV) nuclei of the hypothalamus are densely populated by CART-immunoreactive cells and fibers, whereas anterior hypothalamic nuclei (AHY) as well as lateral hypothalamus (LH) exhibit moderately dense networks of immunoreactive fibers in both LETO (A) and OLETF (B) rats. C and D: Similarly to the LETO (C), in the OLETF rat (D) zona incerta (ZI) expresses a large number of CART immunoreactive neurons, whereas periventricular (PEV) and arcuate (ARC) nuclei contain, in addition to the CART-positive neurons, dense immunoreactive axonal network. Lateral hypothalamic area (LH) contains a less dense network of immunoreactive fibers, and ventromedial hypothalamic nucleus (VMH), as well as dorsal hypothalamic area (DA) displays very low level of immunoreactivity in both LETO (C) and OLETF rats (D). In both strains, very strong immunoreaction is detected in median eminence (ME). E and F: In both LETO (E) and OLETF (F) rats, zona incerta (ZI) and perifornical nucleus (PEF) exhibit numerous strongly stained neurons, whereas periventricular (PEV), arcuate (ARC) and dorsomedial nuclei (DM) contain moderately dense fiber plexus and numerous CART-immunoreactive neurons. Pars compacta of dorsomedial hypothalamic nucleus (DMC), ventromedial hypothalamic nucleus (VMH) and lateral hypothalamic area (LH) exhibit low densities of immunoreactive axons in both LETO (E) and OLETF (F) strains. Similarly to rostral part of hypothalamus, median eminence (ME) reveals the strongest CART peptide immunoreaction in both strains. Antero-posterior coordinates are represented in mm distance from the Bregma (Br). Additional abbreviations: mt, mammillothalamic fascicle; f, fornix. Scale bars = 500 μ m in A–F.

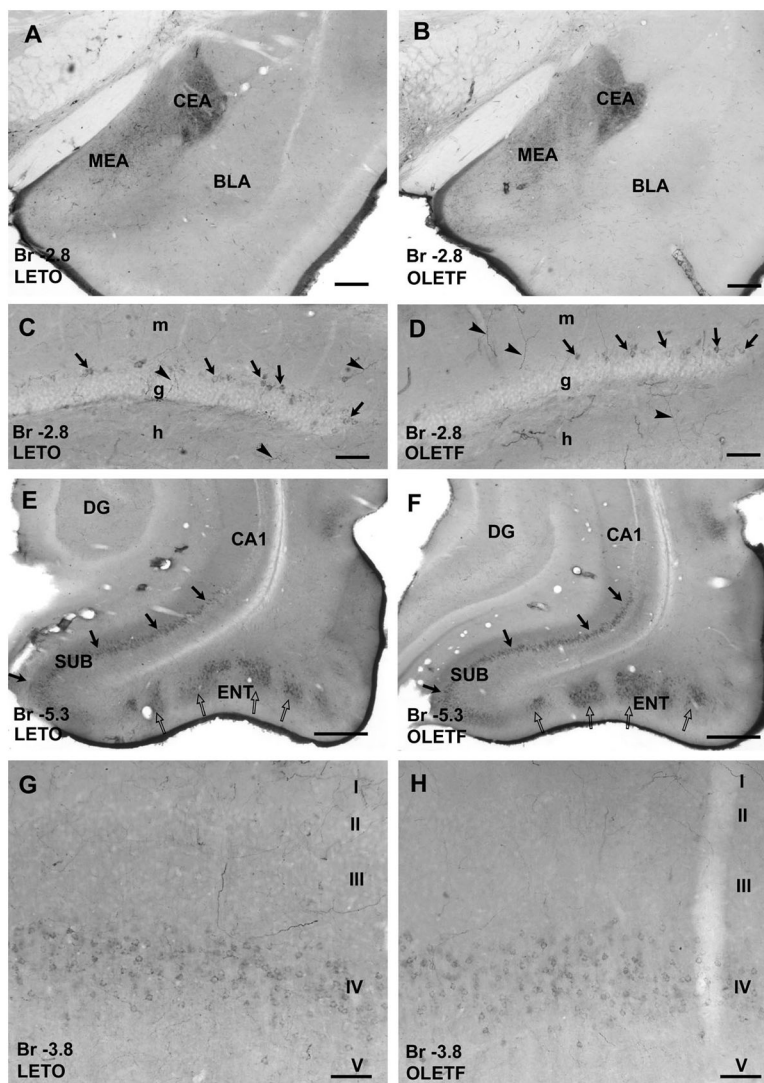


Figure 4. CART peptide immunoreaction in nuclei of amygdala (A and B), in various areas of the temporal archicortex (C–F) and in the somatosensory cortex (G and H) of a lean LETO (A, C, E and G) and an OLETF rat (B, D, F and H). A and B: Large number of CART peptide-immunoreactive neurons and fibers are visible in central nuclei of amygdala (CEA), but density of fibers is moderate in the medial nucleus (MEA) both in LETO (A) and OLETF rats (B). In the rostral part of basolateral amygdala nuclei (BLA) CART-immunoreactive fibers are less dense in the OLETF than in the LETO rat. C and D: CART peptide-immunoreactive granule cells (arrows), dendritic and axonal processes (arrowheads) are visible in the granule cell layer (g) and hilus (h) of the dentate gyrus in both strains. E and F: CART peptide-immunoreactive neurons in the subicular complex (SUB, arrows) and in islets of the entorhinal cortex (ENT, open arrows) in both LETO (E) and OLETF (F) rats. G and H: A large number of faintly immunoreactive neurons was found in layer IV of the somatosensory cortex in both LETO (G) and OLETF (H). Antero-posterior coordinates are represented in mm distance from the Bregma (Br). Additional abbreviations: DG, dentate gyrus; m, molecular layer of the dentate gyrus; CA1, CA1 region of Ammon's horn. Scale bars = 100 μm in C, D, G, H, 200 μm in A and B, 500 μm in E and F.

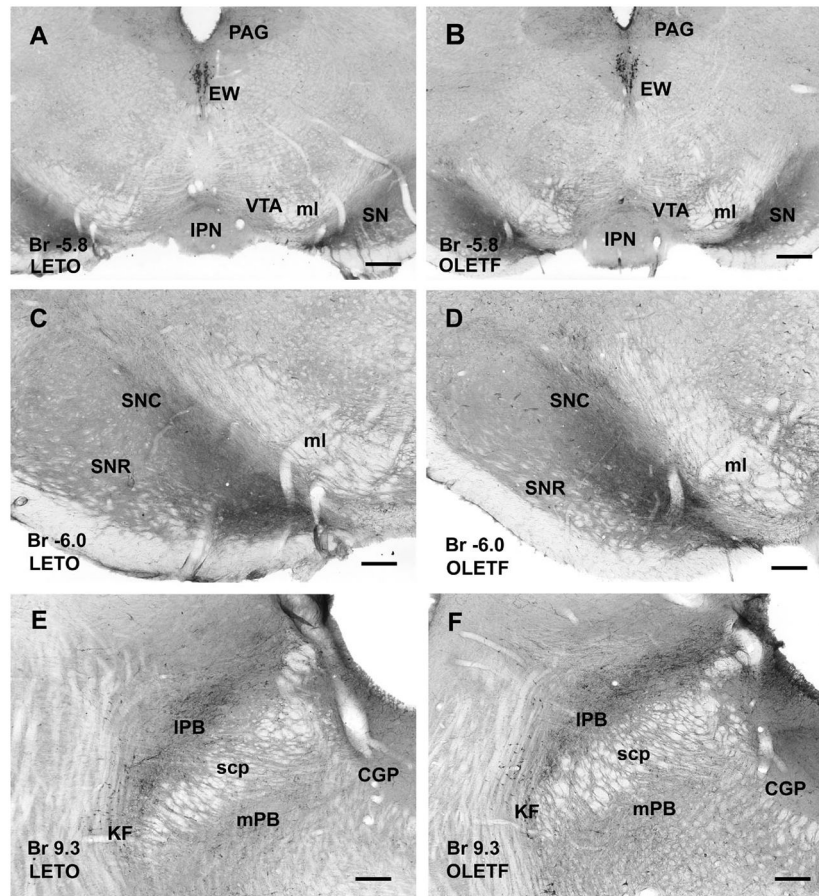


Figure 5. CART peptide-immunoreactive neurons and axonal network in the mesencephalon (AD) and pons (E and F) of LETO (A, C, E) and OLETF rats (B, D, F). A and B: In both strains, the nucleus of Edinger-Westphal (EW) exhibits strongly immunopositive large neurons. In the periaqueductal gray (PAG) moderately dense axonal network is visible, whereas substantia nigra (SN) contains dense CART-immunoreactivity, ventral tegmental area (VTA) exhibits loose networks of CART-immunoreactive fibers in both LETO (A) and OLETF (B) rats. C and D: CART peptide-immunoreactive fibers in both pars reticulata (SNR) and compacta of substantia nigra (SNC) are shown at higher magnification in LETO (C) and OLETF (D) rats. E and F: In the pons, lateral parabrachial nucleus (IPB) contains strongly immunoreactive dense fiber plexus whereas in medial parabrachial nucleus (mPB) as well as in central gray (CGP) CART-immunoreactive axonal density is weaker in both LETO (E) and OLETF (F) rats. CART peptide-immunoreactive neurons are localized in Kolliker-Fuse nucleus (KF) in both strains. Antero-posterior coordinates are represented in mm distance from the Bregma (Br). Additional abbreviation: scp, superior cerebellar peduncle. Scale bar = 500 μ m in A and B, 250 μ m in C–F.

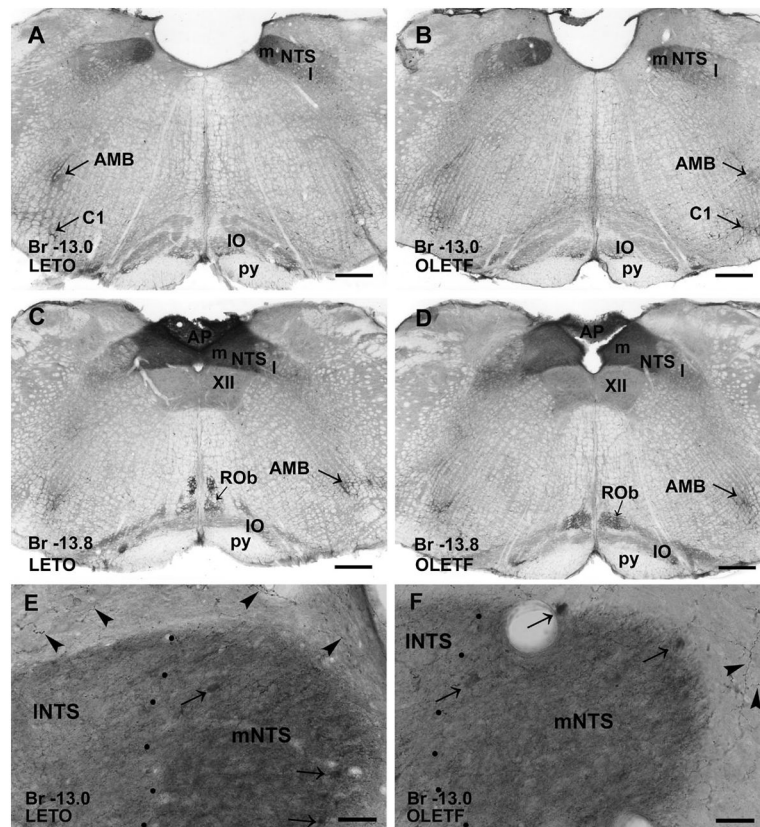


Figure 6.

CART peptide-immunoreactive neurons and axonal networks in the medulla oblongata of a LETO (A, C) and an OLETF (B, D) rat. A and B: The medial part of nucleus of solitary tract (NTS, m) contains dense immunoreactive fiber networks, whereas the lateral part (NTS, l) exhibits lower density of immunoreactive axons and scattered neurons in both LETO (A) and OLETF (B) rats. In the medial nucleus of solitary tract, fibers reveal stronger CART immunoreactivity in LETO than in OLETF rat. In nucleus ambiguus (AMB) and in inferior olive (IO) immunoreactive fibers are detected, and CART peptide containing cells are visible in region of C1 in both lean (A) and obese (B) animals. C and D: Similarly to the rostral level of medulla oblongata, the medial part of nucleus of solitary tract expresses a dense network of immunopositive fibers, while the lateral part contains immunoreactive neurons and moderate density of axons in both strains. In addition, area postrema (AP) exhibits strong CART peptide immunoreactivity. Nuclei raphe obscurus (ROb), ambiguus and oliva inferior express also weak immunopositivity in both LETO (C) and OLETF (D) rats. E and F: Large magnification of the rostral portion of the medial part of nucleus of solitary tract reveals slightly denser fiber plexus in LETO than found in OLETF. Arrows point to CART-immunoreactive neuronal cell bodies. Around the nucleus of the solitary tract strongly CART-immunostained axons (arrowheads) are also visible. Antero-posterior coordinates are represented in mm distance from the Bregma (Br). Additional abbreviation: py, pyramidal tract. Scale bars = 500 μ m in A–D.

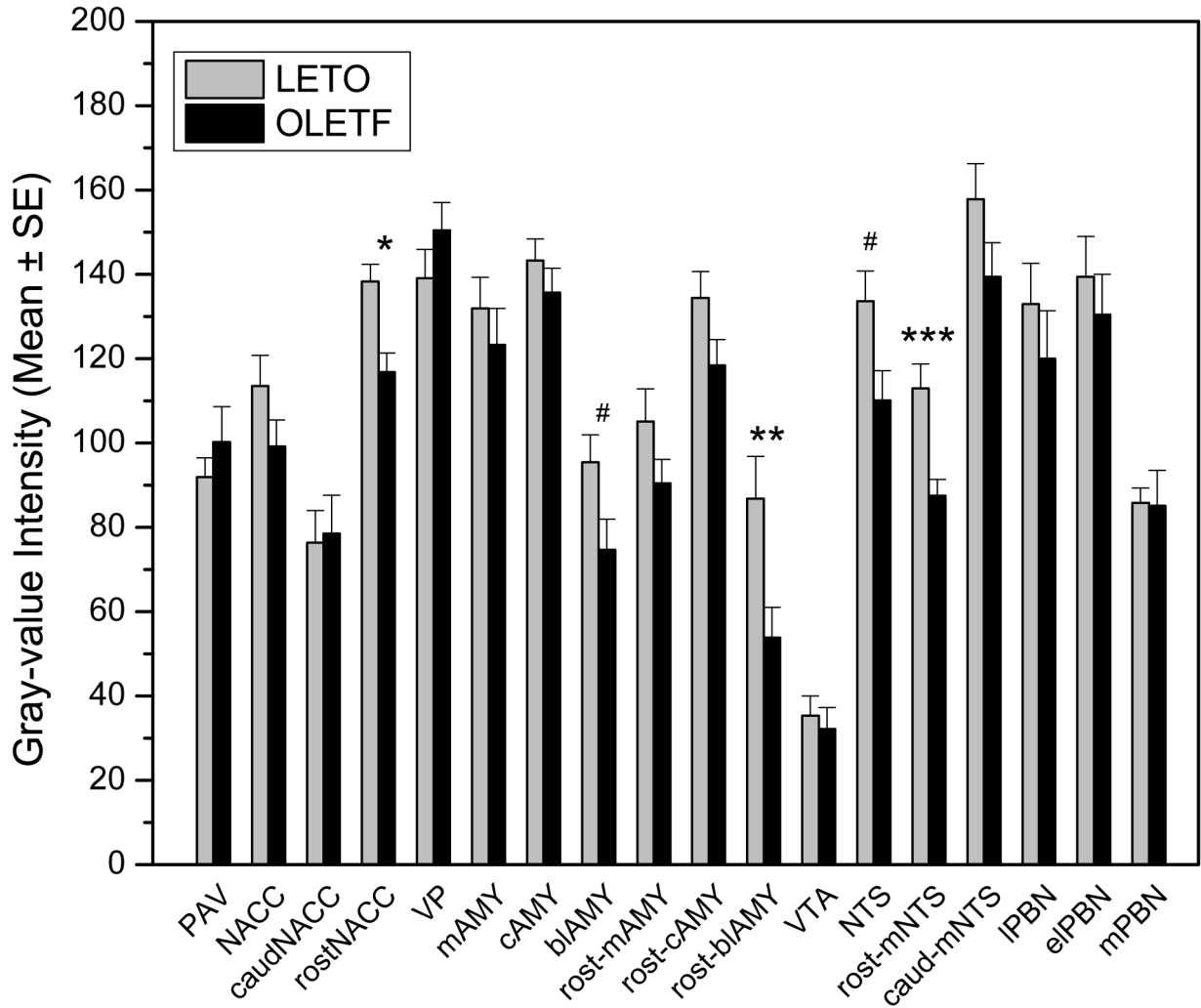


Figure 7.

Summary of data obtained by gray-value intensity measurements for CART immunoreactivity in various brain areas. Open bars represent data from LETO controls, closed bars indicate values obtained in OLETF rats. Additional abbreviations: caudNACC, caudal nucleus accumbens; rostNACC, rostral nucleus accumbens; MEA, medial nucleus of the amygdala; CEA, central nucleus of the amygdala; BLA, basolateral nucleus/complex of the amygdala; rost-MEA, rostral aspect of medial nucleus of the amygdala; rost-CEA, rostral aspect of central nucleus of the amygdala; rost-BLA, rostral aspect of basolateral nucleus/complex of the amygdala; rost-mNTS, rostral portion of the medial part of nucleus tractus solitarii; caud-mNTS, caudal part of the medial part of nucleus tractus solitarii; IPBN, lateral subdivision of the parabrachial nucleus; eIPBN, external lateral subdivision of the parabrachial nucleus, mPBN, medial parabrachial nucleus. # $P < 0.05$; * $P < 0.02$, ** $P < 0.01$, *** $P < 0.001$. Error bars indicate standard error mean.